Astron. Astrophys. 352, 443–446 (1999)

ASTRONOMY AND ASTROPHYSICS

Space-VLBI observations of the twisted jet in 3C 395

L. Lara[1], **A. Alberdi**[1], **J.M. Marcaide**[2], **and T.W.B. Muxlow**[4]

[1] Instituto de Astrofísica de Andalucía (CSIC), Apdo. 3004, 18080 Granada, Spain
[2] Departamento de Astronomía, Universitat de València, 46100 Burjassot, Spain
[3] NRAL, Jodrell Bank, Macclesfield, Cheshire SK11 9DL, UK

Received 8 October 1999 / Accepted 2 November 1999

Abstract. We present Space-VLBI observations of the quasar 3C 395 which show evidence of the existence of a large bend in the inner parts of its jet, close to the core. This bend would explain why previous Earth-based cm-VLBI observations could not detect the ejection of new moving components, as expected from flux density variability in this source. In general, the observational properties of the jet in 3C 395 are heavily marked by the existence of bends on different scales.

Key words: galaxies: active – galaxies: individual: 3C 395 – galaxies: jets – radio continuum: galaxies

1. Introduction

Flux density variability at radio wavelengths in the compact cores of radio loud AGNs on time scales of months or even years is generally associated with ejection of components in parsec-scale relativistic jets (e.g. Valtaoja et al. 1988). Such behavior has been observed in many radio sources (e.g. Pauliny-Toth et al. 1987) and is successfully reproduced by theoretical work (e.g. Hughes et al. 1991, Gómez et al. 1997). However, there are objects which, apparently, do not fit into this scenario. One of these, the quasar 3C 395 ($z = 0.635$), exhibits significant flux density variability which is clearly associated with activity in its compact core (Lara et al. 1994, 1997); however, Very Long Baseline Interferometry (VLBI) observations since 1984 show a stationary morphology, with no evidence of the expected correlation between flux density variability and the ejection of new jet components (Lara et al. 1997).

In this paper we present new VLBI observations of the quasar 3C 395 at 4.8 GHz, made with the Very Long Baseline Array (VLBA) and the Japanese satellite HALCA. These observations not only take profit of the enhanced angular resolution of Space-VLBI, but also of the high sensitivity achieved by the continuous observation of a single source at a single frequency with the VLBA. The new data shed light on the link between flux density variability and the structural properties of 3C 395.

Send offprint requests to: L. Lara (lucas@iaa.es)

2. Observations and data reduction

We made continuum observations of 3C 395 with the VLBA and HALCA on May 1st 1998 at a frequency of 4.8 GHz. The observing bandwidth was 32 MHz. Two tracking stations, Robledo (Spain) and Green Bank (USA), participated in the observations providing maser referenced timing tones to the satellite. At the same time, they received the astronomical data from HALCA through a Ku-band downlink, recording them on magnetic tapes for later processing in a VLBI correlator. In Fig. 1 we display the uv-coverage achieved in our observations to illustrate the improvement in angular resolution provided by the orbiting antenna. The correlation of the data was done *in absentia* by the staff of the VLBA correlator in Socorro (NM, USA). After correlation, we used the NRAO AIPS package to determine the bandpass response functions of the antennas, to correct for instrumental phase and delay offsets between the separate baseband converters in each antenna, to determine antenna-based fringe corrections and to apply the *a priori* amplitude calibration. Data imaging in total intensity was finally performed with the Difmap package (Shepherd et al. 1994).

The imaging process consisted of two main steps: initially, we started mapping the VLBA data alone, i.e. without ground-space baselines, at low angular resolution by reducing the weight of the longer VLBA baselines. Once a satisfactory low resolution map of 3C 395 was obtained, the weight of the long baselines was progressively restored to its original values, so that we finally obtained a map with the VLBA alone at its maximum angular resolution. In this process, we also derived accurate self-calibration solutions for the VLBA antennas. We then included data from HALCA in a second mapping step, improving the source model at sub-milliarcsecond resolution and obtaining a high resolution map from the whole data set. Finally, we calibrated the absolute flux density scale mapping the compact calibrator source 0133+476, also observed during the experiment and with an assumed flux density of 2.50 Jy at 4.8 GHz (information obtained from the University of Michigan Radio Astronomy Observatory (UMRAO) database).

3. Results

Radio maps of 3C 395 are displayed in Fig. 2, with angular resolutions spanning a range from 10 to 0.3 mas.

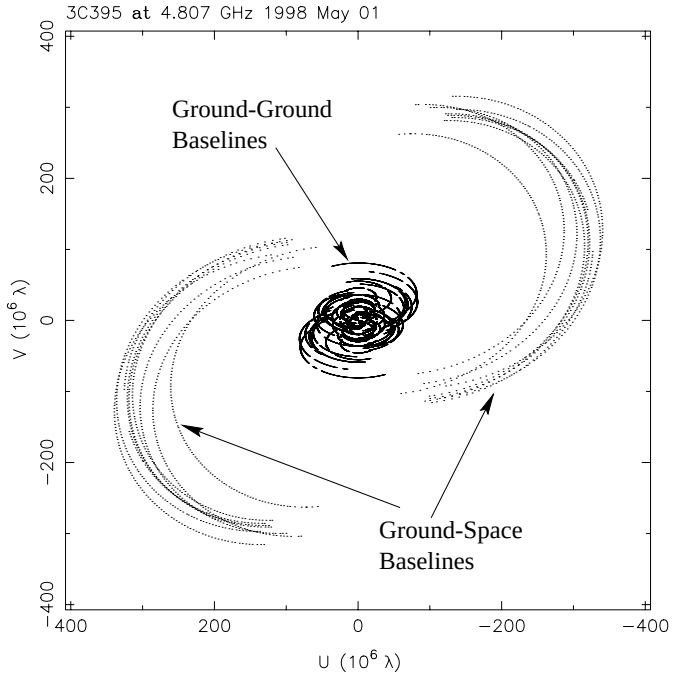

Fig. 1. uv-coverage obtained during the space-VLBI observations presented in this paper. The compact set of uv-data points corresponds to ground – ground baselines. The outer tracks correspond to ground – space baselines. The maximum uv-distance is 384 Mλ.

Fig. 2a shows a low angular resolution map of the jet in 3C 395. The brightness distribution is dominated by a strong double component, but the most remarkable feature at this resolution is the existence of a very sharp bend in the jet at a distance of ∼70 mas from the core. This bend links the compact structure with the extended emission observed at sub-arcsecond resolution (Saikia et al. 1990; Lara et al. 1997). We can follow the jet up to a length of nearly 200 mas thanks to the very high sensitivity of the VLBA. The jet at these large scales is not smooth, but knotty. Two of these knots can be associated to components D and E in Lara et al. (1997). The total flux density recovered in our VLBI observations is 1.43 Jy.

Fig. 2b has an angular resolution similar to that of previously published cm-VLBI maps of 3C 395 (Lara et al. 1994). Leaving apart the weak component D, the radio structure can be described in terms of three main components named A, B and C, as in previous papers. Component A has been usually identified as the radio core; component B appeared stationary with respect to A and was interpreted as the result of a local bend in the jet towards the observer; component C, between A and B, was claimed to be moving superluminally after VLBI observations during the 80's (Waak et al. 1985; Simon et al. 1988a), but no clear evidence of motion was found in later observations (Simon et al. 1988b; Lara et al. 1997).

Figs. 2c-d reveal that a simple description of the compact structure of 3C 395 in terms of only three components is no longer valid when observing with high sensitivity and resolution. Feature A is not a single component: it hosts the core, most plausibly at its western edge, but also a second strong component and a jet-like feature. Such complexity within A was suggested by Lara et al. (1997) after a three-baseline VLBI test observation at 22 GHz. Component B also shows a rather complex structure at high angular resolution. Component C appears resolved (Fig. 2c), and it is difficult to associate it with any single feature, either moving or stationary.

Table 1. VLBI components of 3C 395

Comp.	S (mJy)	D (mas)	P.A. (deg)	L (mas)	r	Φ (deg)
A1	124	0	0	0.59	<0.01	106
A2	629	0.66	109	0.30	0.74	132
A3	245	1.57	126	0.58	0.71	160
C	48	7.60	118	8.70	0.22	118
B1	51	15.18	117	2.45	0.47	170
B2	235	16.09	120	1.65	0.75	66
B3	72	17.60	119	5.63	0.65	116
D	16	48.53	125	7.39	0.80	53

To obtain a quantitative description of the milliarcsecond structure of 3C 395, we have fitted simple elliptical Gaussian components to the visibility data using a least square algorithm within Difmap. We needed a total of 8 components to satisfactorily reproduce the data; we did not attempt to fit the brightness distribution beyond component D along the jet, since this extended emission only marginally affects the data from the shorter baselines. The estimated parameters for each Gaussian component are given in Table 1, where we display the flux density (S), the angular distance from the westernmost component A1 (D), the position angle with respect to A1 (P.A.), the length of the major axis (L), the ratio between the major and minor axis (r) and the orientation of the major axis (Φ), defined in the same sense as the position angle. The elliptical Gaussian components have been plotted on Fig. 4 for direct comparison with the surface brightness distribution.

4. Discussion and conclusions

The launch of satellite HALCA in February 1997 has probably marked an inflection point in the development of radio astronomy. VLBI, continuously improving its sensitivity since its origins in the sixties, has finally managed to break the hard constraints in angular resolution imposed by the limited size of the Earth. As a sample of the new capabilities of VLBI, our observations show that the milliarcsecond structure of 3C 395 is rather more complex than previously thought, with several features which deserve special attention.

First, there is a sudden decrease in the surface brightness of the jet after component A3, defining a sharp boundary between this component and the rest of the jet. Second, the jet position angle between A2 and A3 is 137°, remarkably different from the position angle defined by components C and B (P.A. 118°). These two facts argue towards the existence of a bend in the jet soon after component A3 in which the orientation angle of the jet increases significantly with respect to the observer. Third, as mentioned above, the emission between components

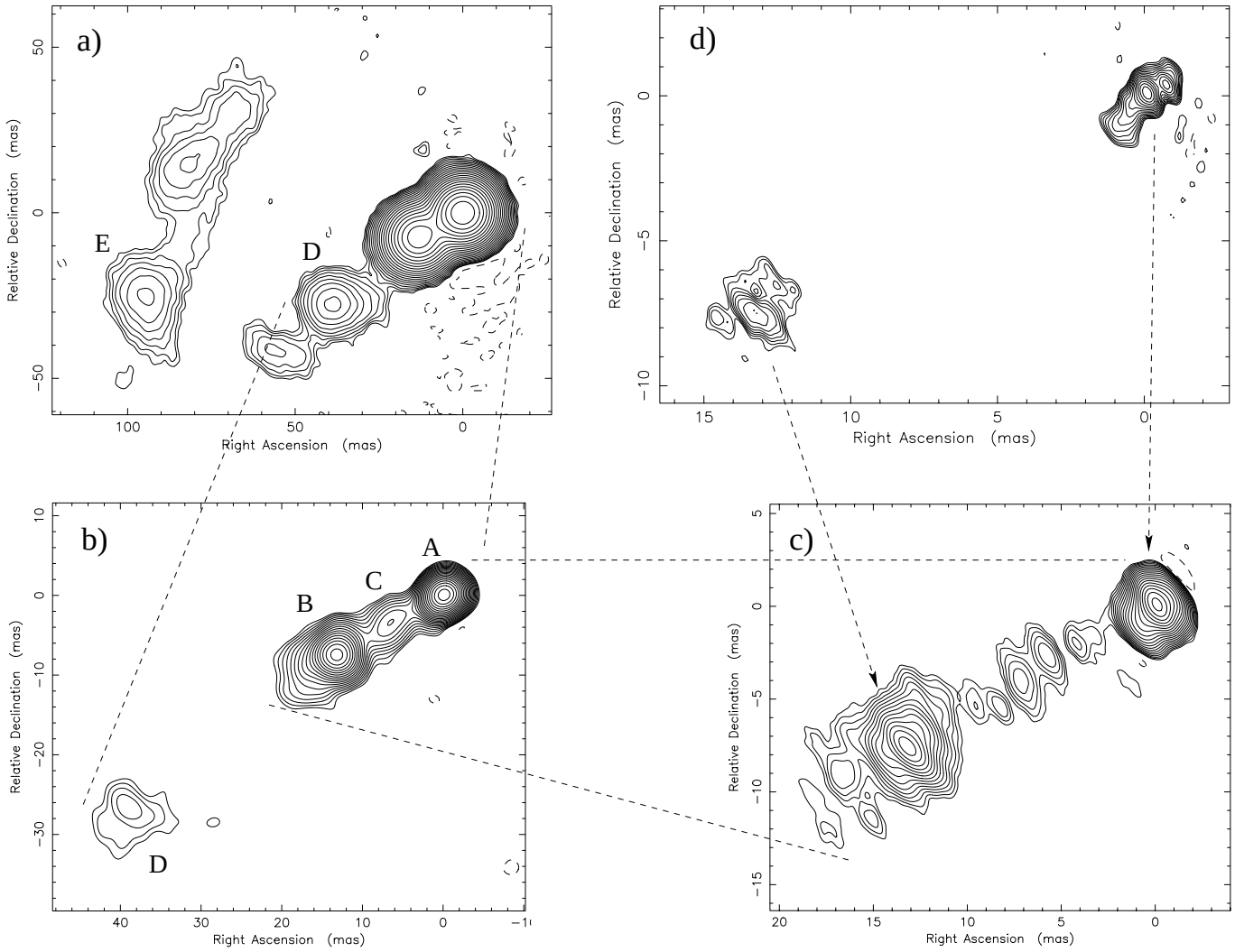

Fig. 2a–d. VLBI maps of the jet in 3C 395 at 4.8 GHz. **a**,**b** correspond to the VLBA alone; **c**,**d** correspond to the VLBA and HALCA. Dashed lines and arrows help to identify equivalent jet regions in the different maps. In all maps contours are spaced by factors of $\sqrt{2}$ in brightness, with the lowest at 3 times the rms noise level. For each map we list the Gaussian beam used in convolution (mas), the rms noise level (mJy beam^{-1}) and the peak of brightness (Jy beam^{-1}). **a**: Beam = 10×10; rms = 0.17; Peak = 1.013; **b**: Beam = 2.5×2.5; rms = 0.24; Peak = 0.894; **c**: Beam = 1.69×0.76 P.A. 31.2°; rms = 0.35; Peak = 0.608; **d**: Beam = 0.67×0.31 P.A. 29.2°; rms = 1.10; Peak = 0.415;

A and B cannot be easily associated with a single component. Nevertheless, in our Gaussian fit we have used only one component to describe this emission in order to compare our results with previous lower resolution observations and look for any evidence of motion, but the Gaussian component we obtain is very elongated, making any motion estimates very uncertain. Moreover, attempts to model the complex structure of C were not conclusive, suggesting that the emission observed between components A and B might be related more to the underlying jet hydrodynamics, rather than to a traveling shocked component.

Another interesting aspect of 3C 395 is related to its variable flux density. In Fig. 3 we display the time evolution in the flux density of 3C 395 at 4.8 and 14.5 GHz since 1982. There are variations of up to 30% in total flux density at both frequencies. Monitoring the quasar with VLBI at several frequencies and angular resolutions since 1990 shows that the flux density variability is related with the activity within component A (Lara et al. 1997).

As noted before, flux density variability in the compact cores of AGNs is usually associated to the ejection of new traveling components along parsec-scale relativistic jets. According to this idea, Fig. 3 suggests that new components should have been ejected from the core of 3C 395 in 1986, 1990 and 1993. However, previous VLBI observations of 3C 395 do not show the expected correlation between flux density variations and the ejection of new VLBI components. The Space-VLBI observations presented here help us to understand this peculiarity: if there exists a large bend in the jet after component A3, it will be very difficult to correlate flux density variability within A with structural variations beyond this component because relativistic time-delay makes the time scales of these two events very different. Moreover, the decrease in the Doppler factor

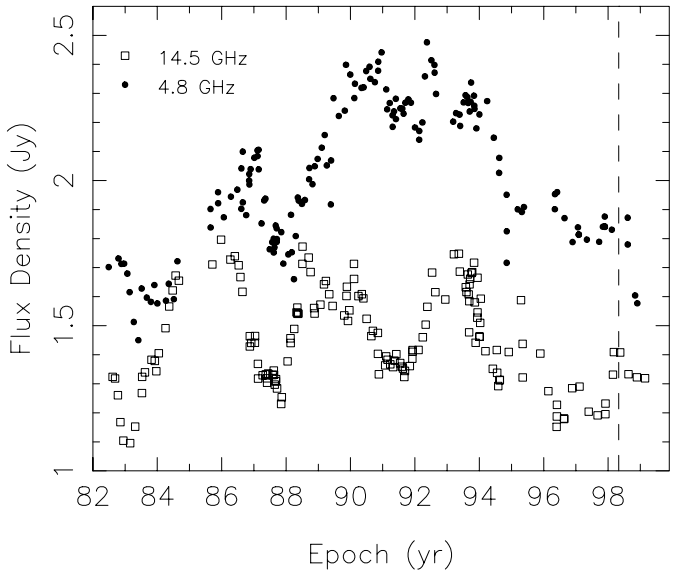

Fig. 3. Time evolution of the flux density of 3C 395 at 4.8 and 14.5 GHz, obtained from the UMRAO database. 8.4 GHz data, also available in this database, have been excluded from this plot for the sake of clarity. The dashed line represents the date of the observations presented here.

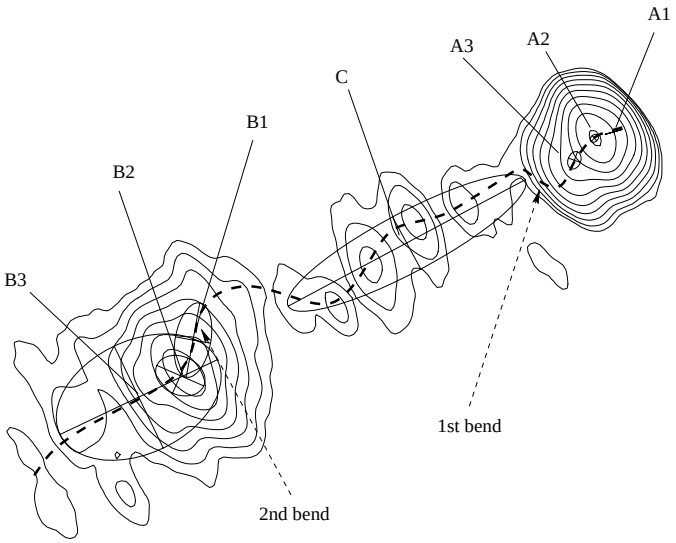

Fig. 4. Space-VLBI image of 3C 395 at 4.8 GHz with an approximate determination of the jet ridge line (dashed line). The positions of the bends which determine the observational properties of 3C 395 are marked. The third sharp bend is out of this plot. Gaussian components in Table 1 are also marked, except component D which lies out of this plot.

after component A3 produces a large diminution in the flux density of a possible moving component. 3C 395 requires submilliarcsecond resolution to study structural variations within A associated to flux density variability. Hence, previous VLBI observations did not have the necessary angular resolution.

The ridge line of the jet of 3C 395 at milliarcsecond scales can be traced from our maps (see Fig. 4) showing the wiggles and curvatures present in this twisted jet. We can conclude that the observed properties of quasar 3C 395 are heavily marked by three main bends which produce changes in the orientation of the jet with respect to the observer, and hence changes in the observed properties due to Doppler factor variations. The first apparent bend, close to the core and producing a departure of the jet direction from the line of sight, might be the reason why flux density flares are not directly followed by ejection of components observable with ground cm-VLBI. The second bend, at 15 mas from the core, orients the jet back towards the observer's line of sight and may be responsible of the Doppler amplification of the emission at this position resulting in the stationary component B. The third bend, at a distance of 70 mas from the core, produces a sharp deflection in the projected ridge line of the jet, appearing to almost turn back upon itself. While the first two bends could possibly be consequence of a helically twisted geometry in the jet (which might explain also components observed beyond B), the third large curvature would require a global bending of the helix. We note that the intrinsic effects of these bends are most probably highly amplified by a sharp overall orientation of the jet in 3C 395 with respect to the observer's line of sight.

Acknowledgements. This research is supported in part by the Spanish DGICYT (PB97-1164). It has made use of data from the University of Michigan Radio Astronomy Observatory which is supported by funds from the University of Michigan. The National Radio Astronomy Observatory is a facility of the National Science Foundation operated under cooperative agreement by Associated Universities, Inc. We gratefully acknowledge the VSOP Project, which is lead by the Japanese Institute of Space and Astronautical Science in cooperation with many organizations and radio telescopes around the world.

References

Gómez J.L., Martí J.M., Marscher A.P., Ibañez J.M., Alberdi A., 1997, ApJ, 482, L33
Hughes P.A., Aller H.D., Aller M.F., 1991, ApJ, 374, 57
Lara L., Alberdi A., Marcaide J.M., Muxlow T.W.B., 1994, A&A, 285, 393
Lara L., Muxlow T.W.B., Alberdi A., et al., 1997, A&A, 319, 405
Pauliny-Toth I.I.K., Porcas R.W., Zensus J.A., et al., 1987, Nature, 328, 778
Saikia D.J., Muxlow T.W.B., Junor W., 1990, MNRAS, 245, 503
Shepherd M.C., Pearson T.J., Taylor G.B, 1994, BAAS, 26, 987
Simon R.S., Hall J., Johnston K.J., et al., 1988a, ApJ, 326, L5
Simon R.S, Johnston K.J., Spencer J.H., 1988b, in The Impact of VLBI on Astrophysics and Geophysics, ed. M.J. Reid & J.M. Moran, Kluwer Academic Publishers, 21
Valtaoja E., Haarala S., Lehto H., et al., 1988, A&A, 203, 1
Waak J.A., Spencer J.H., Johnston K.J., Simon R.S., 1985, AJ, 90(10), 1989